



Natural dyes in hybrid chalcogenide multi-layer thin films

K MILONAKOU-KOUFOUDAKI*, C MITZITHRA, S HAMILAKIS, C KOLLIA and Z LOIZOS

School of Chemical Engineering, National Technical University of Athens, Zografou Campus, 15 780 Athens, Greece

*Author for correspondence (karmenmk@gmail.com)

MS received 18 December 2019; accepted 13 April 2020

Abstract. New highly photoconductive hybrid multi-layer semiconductors have been developed, comprising cathodically electrodeposited CdSe or $Zn_xCd_{1-x}Se$ thin films and natural photosynthetic pigments, isolated from spinach. A layer of the organic dye, Chlorophyll α or Carotenes, is either deposited by spin coating technique over an inorganic thin film (two-layer structures) or 'sandwiched' between two inorganic semiconductive films (three-layer structures). X-ray diffraction, scanning electron microscopy, energy-dispersive X-ray analysis, diffused reflectance spectroscopy and photoelectrochemical studies are employed, in order to fully characterize the received products. In the case of the three-layer hybrids, a significantly enhanced photo-response is observed, leading up to 300% improved photoelectrochemical efficiency values, compared to that of the pure inorganic films. This amelioration, stemming from the synergetic action of hybrids' components, is more prominent in the case of $Zn_xCd_{1-x}Se$ systems, where a significant amount of Cd has been substituted by Zn: therefore, Zn are considered environmentally friendlier alternatives to pure CdSe-based semiconductors.

Keywords. Hybrid materials; thin films; semiconductors; multi-layers; natural dyes; photosensitivity.

1. Introduction

The rapid development of technology and industry, combined with ever-increasing energy demands have created the need for new semiconductors with advanced properties that can lead to innovative applications [1–3]. Under these circumstances, a new class of hybrid materials has been developed, where the coupling of selected organic compounds and inorganic semiconductors in a single system is attempted, in order to develop products with improved properties. It has already been demonstrated that hybrid thin films may significantly differ from their starting materials or even outperform them, often exhibiting a synergistic effect between their inorganic and organic parts. Moreover, a modulation of the end-products' properties can be easily attempted by incorporating specific functional groups in the organic molecules that are introduced to the hybrid semiconductors [4]. These hybrid semiconductive materials may have interesting applications in photovoltaic, photoelectric and optoelectronic devices, as well as in microelectronics, sensors, photodetectors, etc. [5–7].

The present research focuses on the synthesis and study of hybrid (inorganic–organic) semiconductors based on photosynthetic pigments, as alternative, bio-inspired solar energy conversion systems. The main goal is the appropriate and original combination of inorganic thin films that have already demonstrated highly optimized properties in hybrid systems, with organic compounds that are responsible for collecting sunlight during photosynthesis. In particular, the dyes employed here, Chlorophyll α ($Chl\alpha$, $C_{55}H_{72}MgN_4O_5$) and

Carotenes (Crt, mainly $C_{40}H_{56}$), are abundant and non-toxic plant pigments, involved in energy collection, charge separation and electron transfer processes in nature [8–10]. Precisely, because of their natural role as light-harvesting molecules, the selected pigments were expected to add photosensitivity and efficiency to the final system, a fact that is confirmed by this study. This way, pure natural products, that are environmentally friendlier, can replace organometallic compounds that have been used so far to develop multilayer 'sandwich-like' hybrid systems [11].

More specifically, as presented in some of our previous works, hybrid thin films, based on well-known semiconductors, such as CdSe and $Zn_xCd_{1-x}Se$, coupled with commercially available compounds like ferrocene (Fc) and ferrocene aldehyde (FcCHO), present remarkably improved photoresponding behaviour. Detailed studies have been conducted regarding the electrochemical formation, as well as the photoresponse of CdSe. This semiconductor, with direct bandgap (1.7 eV) and a large optical absorption range, has already found many applications in thin film solar cells. Furthermore, its 'kindred' mixed semiconductor $Zn_xCd_{1-x}Se$, though less photoactive, is more resistant against photocorrosion and provides the additional advantage of bandgap modulation by composition (1.7–2.7 eV) [12]. Thus, an attempt is made to shift towards such ternary systems, based on the premise that an increased solar spectrum sensitivity and good stability can be accomplished at the same time. Additionally, due to the fact that cadmium is a metal that its toxicity has raised several concerns over the years, its partial replacement with zinc in $Zn_xCd_{1-x}Se$ systems is considered to be a step towards

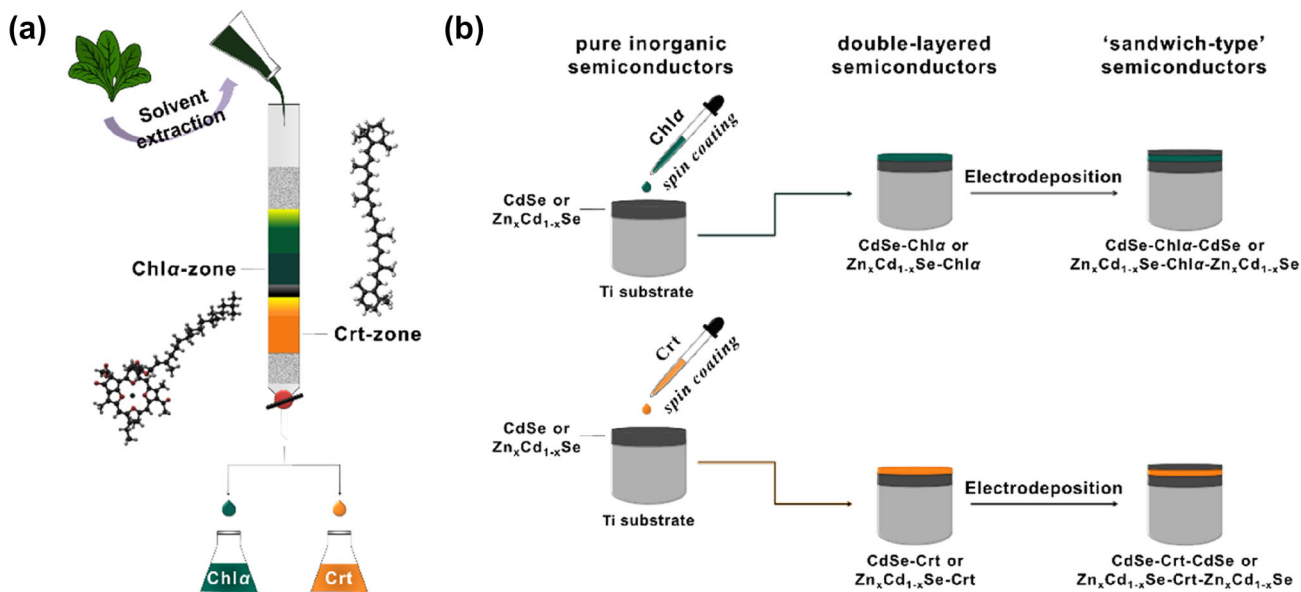


Figure 1. (a) Schematic representation of Chl α and Crt isolation process and (b) illustration of the hybrid samples' structure and fabrication.

producing more cost-efficient and eco-friendlier semiconductors [13–15]. The interaction of Chl α and Crt with CdSe and Zn $_x$ Cd $_{1-x}$ Se thin films, the examination of the induced changes in the systems and the prospects of the resulting hybrids are being investigated here for the first time, as evidenced by the recent literature, and therefore constitute a new research field.

2. Experimental

2.1 Natural dyes' isolation from spinach

The primary step of the hybrids' fabrication was the isolation of the dyes from an inexpensive natural source through a simple and rapid solvent extraction method, followed by silica gel column chromatography, according to literature [16–20]. More specifically, Chl α and Crt were simultaneously extracted from freeze-dried spinach, one of the most common vegetables used for their isolation [21,22], among other sources [23,24]. The isolated pigments were identified *via* standard UV–Vis Spectroscopy, giving clear spectra with the expected characteristic peaks [25,26]. Each pure dye was then dissolved in acetone in order to form a clear solution to be used in the fabrication of the hybrids, as described below.

2.2 Development of the hybrid systems

The hybrid thin films consist of two or three alternating layers. In more detail, the two-layer specimens consist of an inorganic thin film coated with a layer of the organic dye, while, in the case of the three-layer systems, the two

inorganic semiconductive films are separated by an intermediate layer of the photosynthetic dye, forming a 'sandwich' structure. First, the inorganic CdSe or Zn $_x$ Cd $_{1-x}$ Se thin film ('inner' layer) was cathodically electrodeposited onto a titanium (Ti) substrate from an electrolytic bath that contains typically: (1) 0.2 M CdSO $_4$ and 2 mM SeO $_2$ for CdSe plating or (2) 0.2 M ZnSO $_4$, 0.2 mM CdSO $_4$ and 0.2 mM SeO $_2$ for Zn $_x$ Cd $_{1-x}$ Se plating. More details regarding the electrodeposition conditions and experimental setup can be found in previous reports [12]. It is noted that in this study all CdSe thin films of all specimens were electrodeposited at -1.0 V *vs.* S.S.E. (Hg|HgSO $_4$ saturated sulphate reference electrode), whereas Zn $_x$ Cd $_{1-x}$ Se thin films at -1.2 V *vs.* S.S.E., respectively.

Subsequently, the selected organic dye (Chl α or Crt) was spin-coated onto the surface of the inorganic semiconductor from its acetone solution, forming the second or intermediate layer. Finally, when the 'sandwich' hybrids were prepared, a third 'outer' layer of the same semiconductor (CdSe or Zn $_x$ Cd $_{1-x}$ Se) was electrodeposited over the dye, under the same above-mentioned conditions. Total thickness of the three-layered systems was calculated to be approximately 4–5 μ m. Pure inorganic CdSe and Zn $_x$ Cd $_{1-x}$ Se thin films, as well as the respective double-layered specimens coupled with each dye were also prepared, studied and included in this work, for reference. Both isolation and hybrid systems' fabrication procedures are demonstrated in figure 1.

The layer structure of all synthesized and investigated samples is summarized in table 1. To facilitate comparison of the experimental data and results, an appropriate abbreviation (sample abbrev.) has been assigned to each sample and

Table 1. Overview of layer structure of the synthesized inorganic and hybrid thin films.

Sample abbrev.	1st Layer ('inner' inorganic layer)	2nd Layer (organic layer)	3rd Layer ('outer' inorganic layer)
CS	CdSe	—	—
CS-Chl α	CdSe	Chl α	—
CS-Chl α -CS	CdSe	Chl α	CdSe
CS-Crt	CdSe	Crt	—
CS-Crt-CS	CdSe	Crt	CdSe
ZCS	Zn $_x$ Cd $_{1-x}$ Se	—	—
ZCS-Chl α	Zn $_x$ Cd $_{1-x}$ Se	Chl α	—
ZCS-Chl α -ZCS	Zn $_x$ Cd $_{1-x}$ Se	Chl α	Zn $_x$ Cd $_{1-x}$ Se
ZCS-Crt	Zn $_x$ Cd $_{1-x}$ Se	Crt	—
ZCS-Crt-ZCS	Zn $_x$ Cd $_{1-x}$ Se	Crt	Zn $_x$ Cd $_{1-x}$ Se

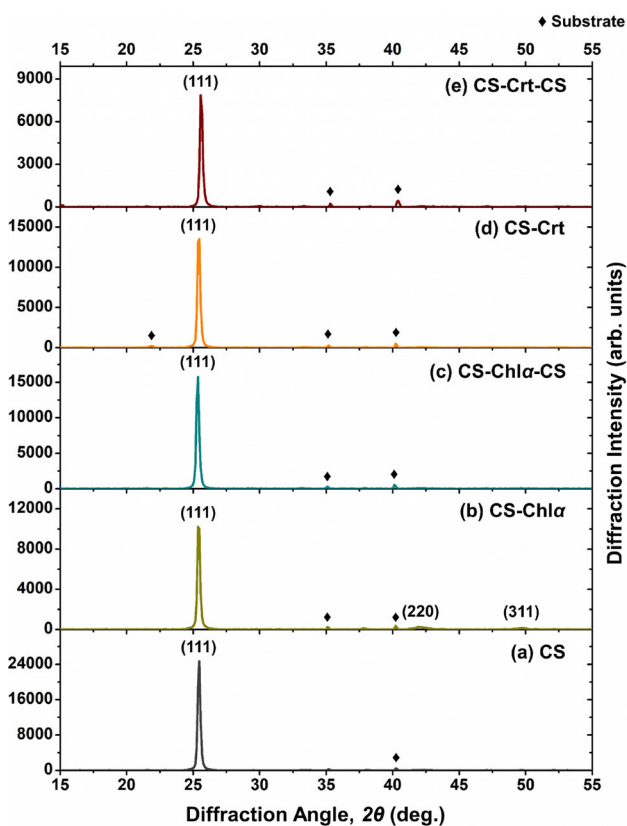


Figure 2. XRD patterns of CdSe-based inorganic and hybrid thin films corresponding to samples (a) CS, (b) CS-Chl α , (c) CS-Chl α -CS, (d) CS-Crt and (e) CS-Crt-CS.

is used hereafter in the text, tables and figures throughout 'Results and discussion' and 'Conclusions' sections.

X-ray diffraction (XRD; Bruker D8 Advance with CuK α X-ray source) was used in order to determine the crystallographic structure of all deposits, and scanning electron microscopy (SEM; Jeol JSM-6390) to examine their surface morphology. Energy-dispersive X-ray analysis (EDAX) was utilized to obtain compositional data and determine

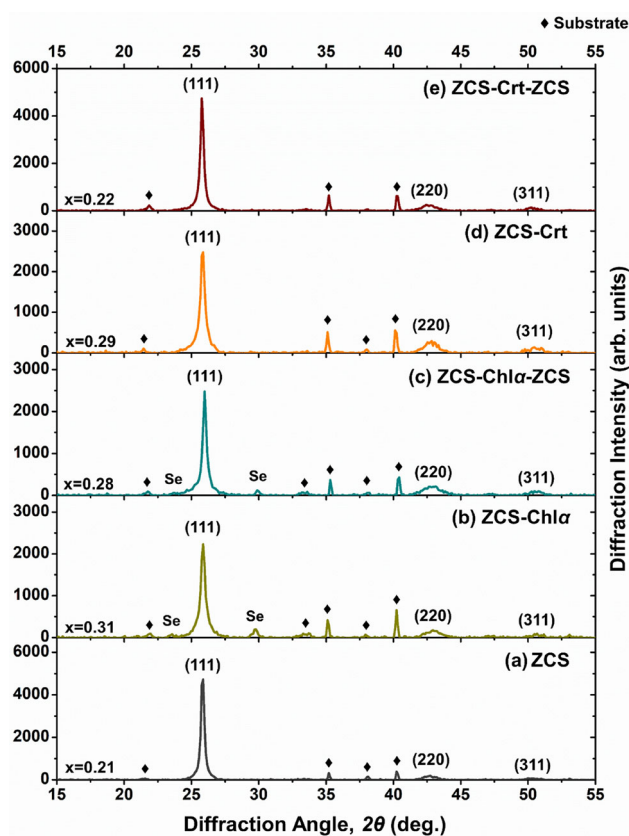


Figure 3. XRD patterns of Zn $_x$ Cd $_{1-x}$ Se-based inorganic and hybrid thin films corresponding to samples (a) ZCS, (b) ZCS-Chl α , (c) ZCS-Chl α -ZCS, (d) ZCS-Crt and (e) ZCS-Crt-ZCS. The mole fraction (x) is provided for each sample according to EDAX investigation (refer to figure 4 and table 3).

molar fraction (x) in the case of Zn $_x$ Cd $_{1-x}$ Se samples. In order to directly determine the optical absorption edge and respective bandgap widths (E_g) of the samples, diffused reflectance spectroscopy (V-770 Jasco spectrophotometer, equipped with 60 mm integrating sphere ISV-922/ISN-901i)

Table 2. Calculated values of micro-structural parameters of the synthesized inorganic and hybrid thin films.

Sample abbrev.	2θ (deg.)	β (deg.)	a (Å)	d_{hkl} (Å)	D_{hkl} (nm)	ε ($\times 10^{-3}$)	δ ($\times 10^{14}$ lines m^{-2})
CS	25.42	0.173	6.06	3.50	49.1	3.35	4.15
CS-Chl α	25.40	0.163	6.07	3.50	52.2	3.15	3.67
CS-Chl α -CS	25.33	0.196	6.08	3.51	43.4	3.81	5.32
CS-Crt	25.41	0.172	6.06	3.50	49.3	3.33	4.11
CS-Crt-CS	25.59	0.178	6.02	3.48	47.7	3.42	4.39
ZCS	25.81	0.266	5.97	3.45	32.0	5.06	9.77
ZCS-Chl α	25.91	0.422	5.95	3.43	20.2	7.99	24.53
ZCS-Chl α -ZCS	25.87	0.355	5.96	3.44	24.0	6.74	17.36
ZCS-Crt	25.81	0.422	5.97	3.45	20.2	8.04	24.62
ZCS-Crt-ZCS	25.82	0.288	5.97	3.45	29.6	5.47	11.42

was employed. A bare titanium disk served as the reflectance standard. Finally, photoelectrochemical studies were conducted utilizing a sulphide-polysulphide solution under a white illumination (1000 W m^{-2}), as described in detail in previous studies [4,12].

3. Results and discussion

According to the XRD patterns received and presented in figures 2 and 3, all deposits exhibit a zincblende structure. It is known that both CdSe and $\text{Zn}_x\text{Cd}_{1-x}\text{Se}$ semiconductors can be found in wurtzite (hexagonal), as well as in zincblende (cubic) form, but it has been observed that an electrochemical deposition route results, almost exclusively, in products of cubic structure.

Additionally, it is found that (111) crystalline orientation, which is known to predominate over (220) and (311) orientations for electrodeposited inorganic zinc and cadmium selenides prepared under the investigated experimental conditions, is also the preferable one for all hybrid samples and the overall picture is clearly retained. Regarding inorganic and hybrid $\text{Zn}_x\text{Cd}_{1-x}\text{Se}$ samples, all diffraction peaks shift towards larger angles compared to CdSe values (JCPDS No. 65-2891; i.e., ZnSe values (JCPDS No. 05-0522)), which is an indication of the formation of the ternary system, in accordance with previous studies [12]. Finally, the fact that the presence of elemental selenium (JCPDS No. 42-1425), which only appears in hybrid samples ZCS-Chl α -ZCS and ZCS-Crt-ZCS, is particularly limited, as indicated by the low intensity of the relative peaks, is encouraging (figure 3b and c).

Average crystallite size and other micro-structural parameters were estimated and are listed in table 2, taking into account the most preeminent (111) orientation observed in all XRD patterns. The values calculated from the reflection data corresponding to the (111) dominant plane were deemed more reliable, due to the anisotropic growth of the samples and the generally low intensity of the (220) and (311) peaks observed in high angles.

More specifically, the X-ray line broadening method was employed in order to obtain the average crystallite size (D_{hkl}) for the preferred plane (hkl) according to the Debye-Scherrer's formula:

$$D_{hkl} = \frac{K\lambda}{\beta \cos \theta}, \quad (1)$$

where β is the full-width at half-maximum (FWHM) intensity of the respective diffraction peak, λ the wavelength of the X-ray radiation used (1.54 \AA), θ the Bragg angle and K a shape factor known as Scherrer's constant, the most common value of which is 0.94 for spherical crystals with cubic symmetry. Instrumental broadening was not taken into account [27].

Interplanar spacing (d_{hkl}) was determined from the Bragg's law:

$$d_{hkl} = \frac{\lambda}{2 \sin \theta} \quad (2)$$

and used to calculate the lattice constant (a) according to the following simple relation, applied for cubic symmetry [28]:

$$a_{\text{cubic}} = d_{hkl} \sqrt{h^2 + k^2 + l^2} \quad (3)$$

where h , k and l are the Miller indices.

Based on the estimated D_{hkl} values, dislocation density (δ) was also determined by the Williamson and Smallman's formula [29]:

$$\delta = \frac{1}{D_{hkl}^2}. \quad (4)$$

Finally, micro-strain (ε) was obtained using the formula [30,31]:

$$\varepsilon = \frac{\beta}{4 \tan \theta}. \quad (5)$$

Table 3. Compositional data of $Zn_xCd_{1-x}Se$ -based inorganic and hybrid thin films estimated using EDAX data.

Sample abbrev.	ZCS	ZCS-Chl α	ZCS-Chl α -ZCS	ZCS-Crt	ZCS-Crt-ZCS
Mole fraction, x	0.21	0.31	0.28	0.29	0.22

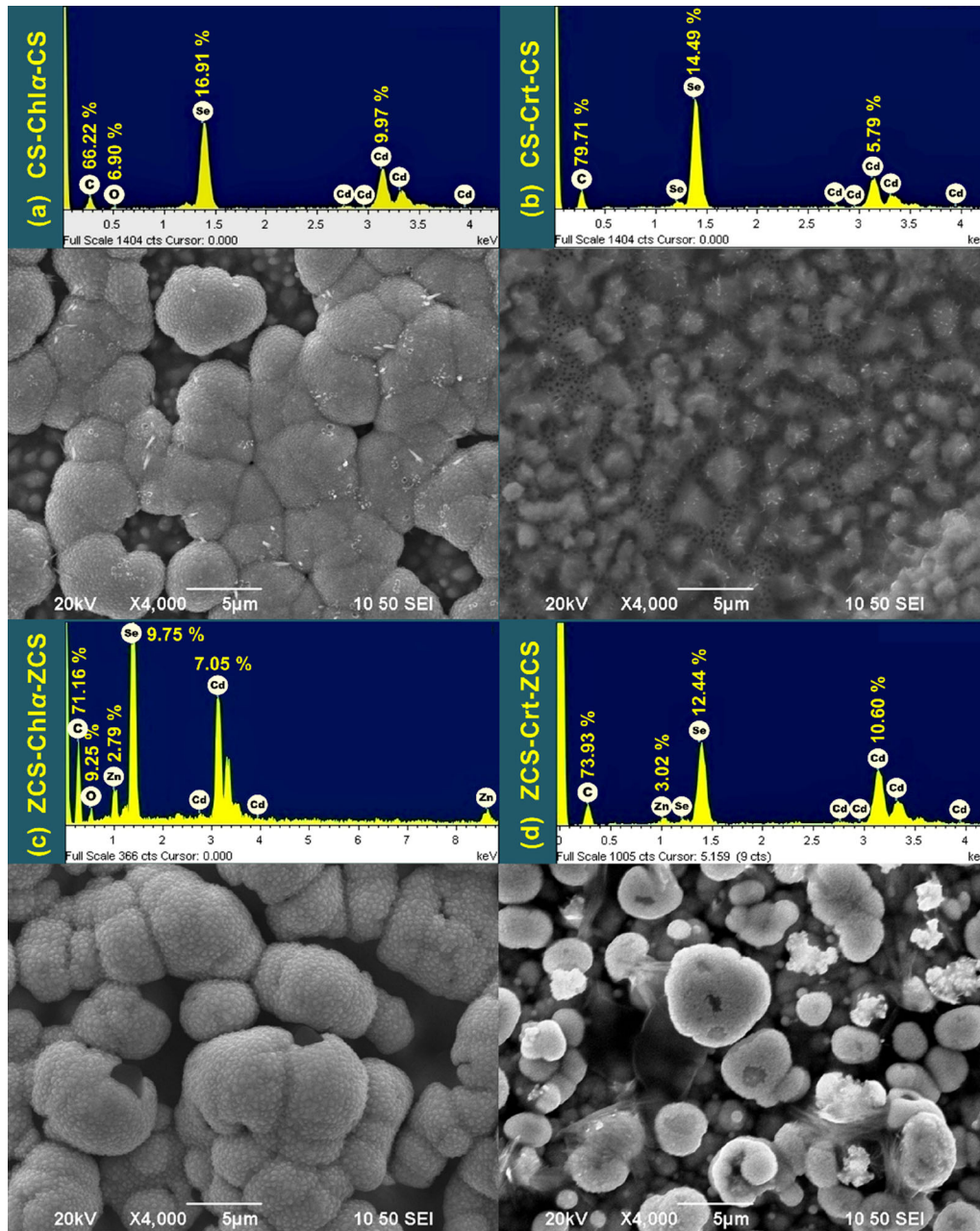


Figure 4. SEM micrographs and EDAX diagrams of hybrid thin films corresponding to samples (a) CS-Chl α -CS, (b) CS-Crt-CS, (c) ZCS-Chl α -ZCS and (d) ZCS-Crt-ZCS.

Estimated crystallite size for all specimens is of the nanometre scale, ranging from ~ 50 to ~ 20 nm. It is noted that the incorporation of zinc in the CdSe lattice in the case

of $Zn_xCd_{1-x}Se$ samples results in an expected crystallite size reduction, regarding both inorganic and hybrid specimens. Correspondingly, dislocation density and micro-strain values

are increased. These changes appear to be proportional to the zinc content of the films, with samples having minimum crystallite size (ZCS-Chl α and ZCS-Crt) also having maximum zinc incorporation (refer to table 3). The results are in good agreement with respective calculations found in the literature for zinc and cadmium selenides using the same equations [32]. The dependence of micro-structural parameters on hybridization is not clear and requires further investigation, because the tendency of Zn $_x$ Cd $_{1-x}$ Se-based hybrid samples to have lower D_{hkl} and higher δ and ε values than the inorganic Zn $_x$ Cd $_{1-x}$ Se film coincides with the abovementioned zinc content increase and a relative decrease does not systematically appear in the case of CdSe-based specimens. The possibility that these two factors simultaneously affect the end result cannot be ruled out. The nature of the organic dye used for the preparation of the hybrids does not seem to dramatically affect the investigated structural properties, although Chl α may lead to lower D_{hkl} and higher δ and ε values than Crt based on the current data for the three-layered samples.

Figure 4 displays SEM micrographs of the hybrid samples, as well as the corresponding spectra and compositional data obtained using EDAX. As shown, all deposits are characterized by ‘cauliflower’ morphology. However, they present some noticeable differences, depending on the nature of the organic compound, which has been used for their preparation. It is observed that Chl α -containing samples, either CdSe or ZnCdSe-based, present a fairly similar surface morphology with a relative uniform distribution of grains that are packed not too tightly together in some surface areas, resulting in a limited, nevertheless noticeable, number of voids in the outer layer deposit, especially in the case of CS-Chl α -CS sample. Crt-containing samples, on the other hand, present a completely different picture. CS-Crt-CS sample clearly shows the most homogeneous, compact and dense surface morphology of all specimens, exhibiting smaller, closely packed, grains with no cracks or pinholes on the film’s surface. In contrast, SEM investigation of ZCS-Crt-ZCS sample reveals that the surface of the film consists of spherical grains, well separated from each other, with an uneven size distribution.

EDAX investigation confirms a high carbon presence in the hybrids (~70% in average), also easily detectable as dark grey areas in the micrographs. Finally, mole fraction (x), calculated using EDAX data for Zn $_x$ Cd $_{1-x}$ Se films and listed in table 3, ranges between 20 and 30% that is considered adequate with respect to the applied method and conditions.

Spectrophotometry studies were conducted in order to identify the isolated pigments and are presented in figure 5. More specifically, the diffuse reflectance spectra of pure Chl α and Crt thin films are given in figure 5b and c and the absorbance spectra of their solutions in acetone in figure 5a.

A direct determination of the absorption edges and the relative bandgap energies of the developed semiconductive materials was achieved through the evaluation and appropriate graphic processing of their diffuse reflectance spectra. Each absorption edge observed corresponds to a point at which

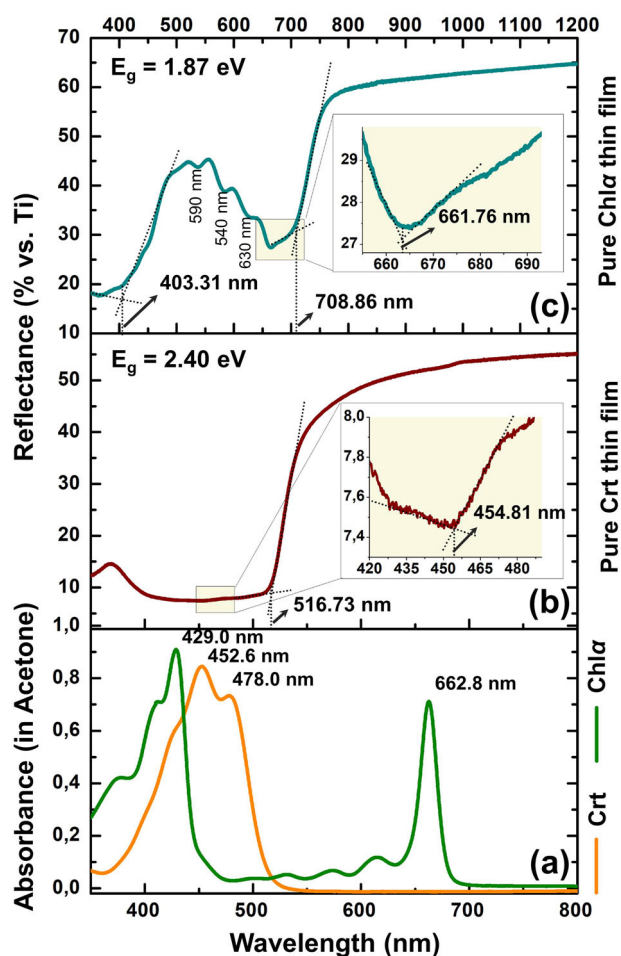


Figure 5. (a) Absorbance spectra of pure Chl α and Crt solutions in acetone and reflectance spectra of pure (b) Crt and (c) Chl α thin films spin-coated onto Ti substrates, evidencing the direct calculation of their bandgap energy values (E_g).

reflection sharply decreases and is determined by the intersection of two lines, as indicated in figures 5 and 6. The first line drawn is tangent to the linear region of the curve where the slope is maximized, while the second is tangent to the base line at wavelengths near the transition region. The determined wavelength (λ_{max}) that corresponds to the absorption edge is converted into bandgap energy (E_g) according to the relationship:

$$E = h\nu = \frac{hc}{\lambda} = \frac{1240}{\lambda}, \quad (6)$$

where E is the photon energy (eV), ν the frequency (Hz) and λ (nm) the wavelength of the incident light, h is Planck’s constant (4.1357×10^{-15} eV s) and c the speed of light (3×10^{17} nm s $^{-1}$).

The reflectance spectra of pure Chl α and Crt thin films applied onto titanium substrates display three and two main

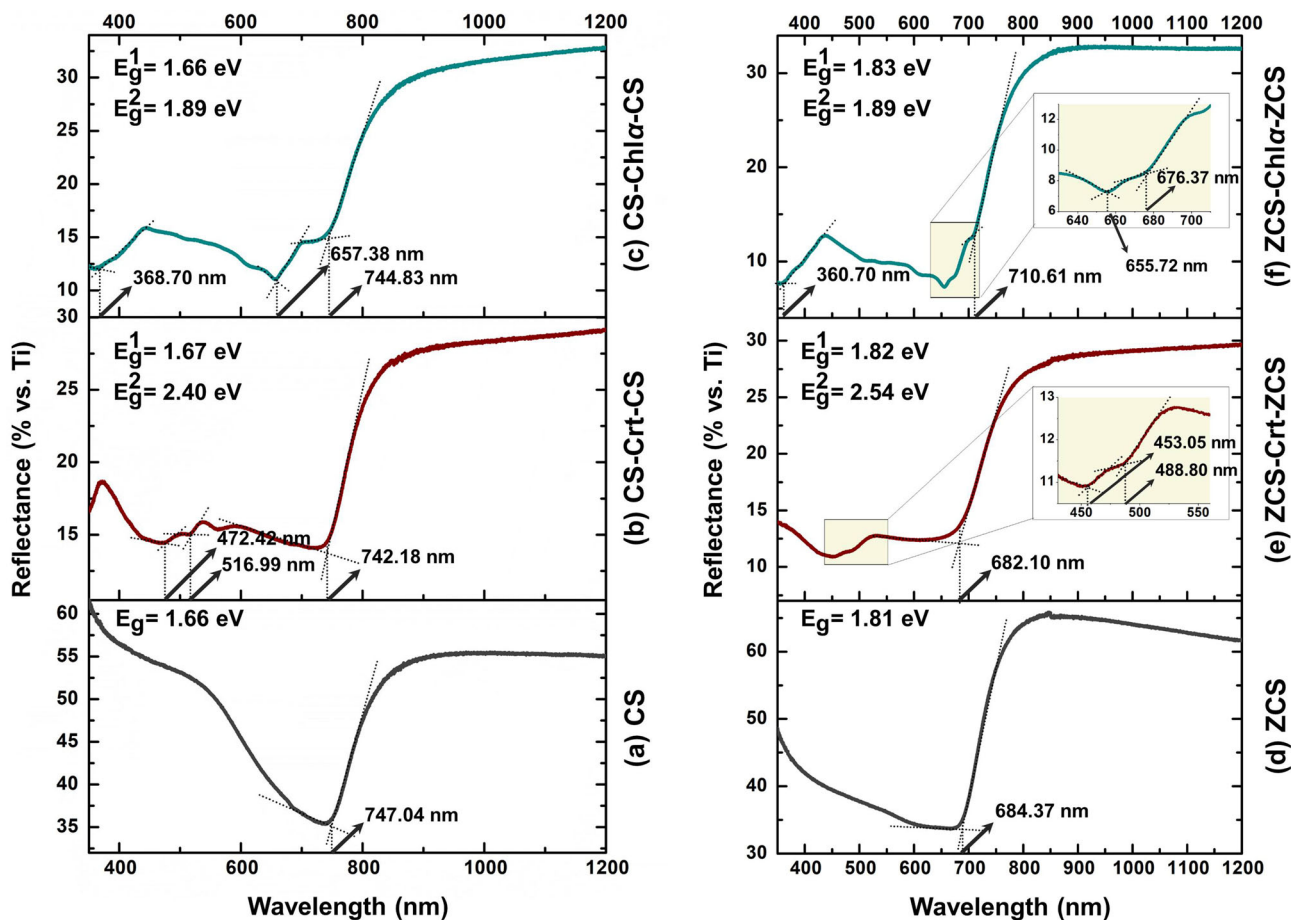


Figure 6. Reflectance spectra of synthesized thin film samples: (a) CS, (b) CS-Crt-CS, (c) CS-Chl α -CS, (d) ZCS, (e) ZCS-Crt-ZCS and (f) ZCS-Chl α -ZCS, evidencing the direct calculation of their bandgap energy values (E_g).

transitions, respectively, consistent with literature [33–36], as shown in figure 5b and c. These transitions, attributed to the presence of the organic dyes, are also observed in the reflectance spectra of the three-layered samples, as shown in figure 6b, c, e and f, confirming the hybridization.

Bandgap energy values were also estimated by diffuse reflectance data analysis according to the Kubelka–Munk approach. In more detail, the analogous Tauc plots for all inorganic and hybrid samples were obtained by applying the Kubelka–Munk theory, expressed by the following equation:

$$[F(R) hv]^{1/n} = A(hv - E_g), \tag{7}$$

where hv is the incident photon energy, n a coefficient associated with the nature of the electronic transition and equal to $1/2$ in the case of direct allowed transitions, A is a proportionality constant, E_g the optical bandgap energy and $F(R)$ the Kubelka–Munk function given by the formula [37–40]:

$$F(R) = \frac{(1 - R)^2}{2R}, \tag{8}$$

where R is the diffuse reflectance.

The modified Kubelka–Munk function $[F(R)hv]^2$ was plotted against photon energy (hv) for each inorganic and hybrid sample and is shown in figure 7. The relative E_g values derived from the intersection points of the extrapolated linear parts of the curves related to the absorption edges and the baselines drawn near each threshold, based on the lowest energy linear segments that precede the transitions [41–44]. By taking into account these linear parts below and above the absorption tail, it is possible to avoid an underestimation of the E_g values, which can be observed, especially in relation with hybrid samples that contain more than one optical absorbing materials and, thus, multiple edges in a single graph [45–47].

The resulting E_g values applying both methods are listed in table 4. Comparing the results, the calculated values are in most cases identical or very close. However, it should be noted that the observed transitions are generally more acute in the reflectance spectra compared to the respective Tauc plots and the sharper slopes, combined with a better xy -aspect ratio, may reduce subjectivity in the calculations.

According to both methods, the hybrids’ spectra exhibit one main transition corresponding to that of the inorganic

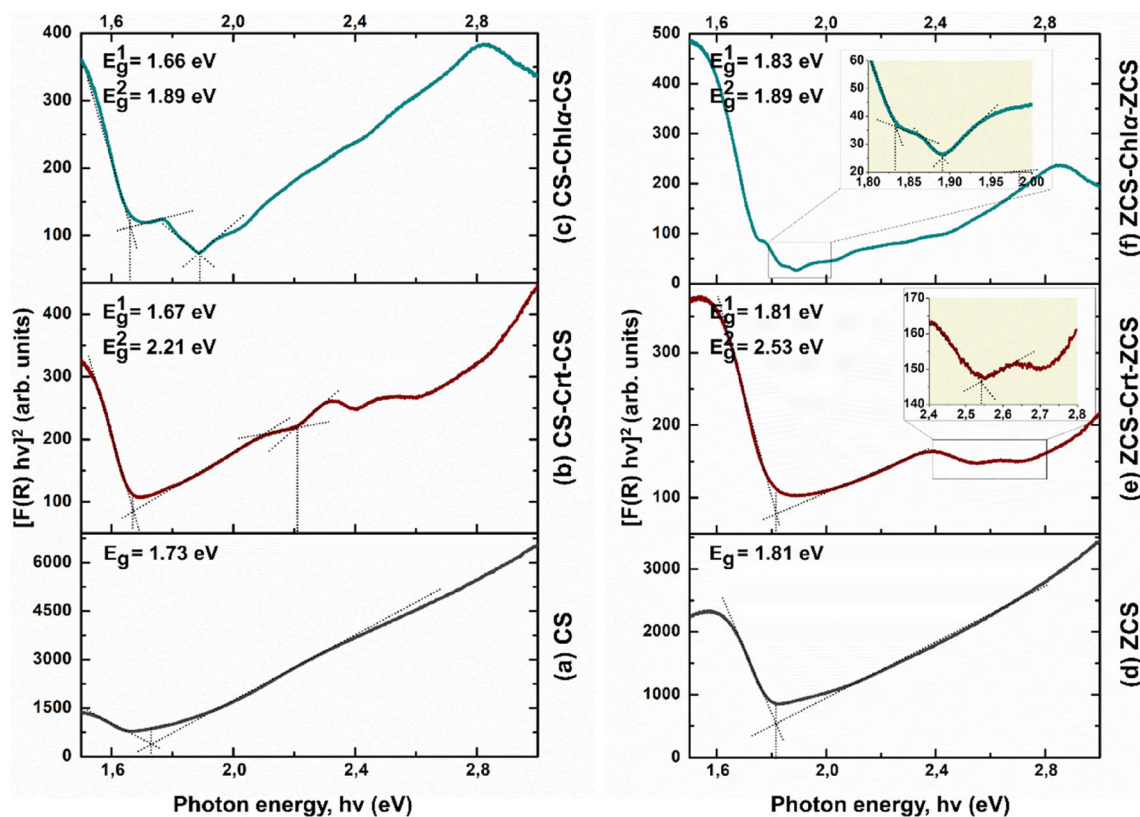


Figure 7. Tauc plots of the modified Kubelka–Munk function $[F(R)hv]^2$ vs. photon energy (hv) of synthesized thin film samples: (a) CS, (b) CS-Crt-CS, (c) CS-Chl α -CS, (d) ZCS, (e) ZCS-Crt-ZCS and (f) ZCS-Chl α -ZCS.

Table 4. Bandgap energy values estimated by (a) direct graphic processing of the samples' diffuse reflectance spectra and (b) application of the Kubelka–Munk approach.

Sample abbrev.	Direct reflectance spectra graphic processing		Kubelka–Munk approach	
	E_g^1	E_g^2	E_g^1	E_g^2
CS	1.66	—	1.73	—
CS-Chl α -CS	1.66	1.89	1.66	1.89
CS-Crt-CS	1.67	2.40	1.67	2.21
ZCS	1.81	—	1.81	—
ZCS-Chl α -ZCS	1.83	1.89	1.83	1.89
ZCS-Crt-ZCS	1.82	2.54	1.81	2.53

semiconductor (E_g^1) at about 1.7 eV (CdSe films) or 1.8 eV (Zn_xCd_{1-x} Se films), accompanied by a number of secondary edges. In more detail, regarding pure Chl α thin films and Chl α containing hybrid samples, the sharp decrease in reflectance known as the 'red edge' is observed in the relative spectra around 710 nm, which is in good agreement with previous reports [48–50]. It is noted that, in the case of CS-Chl α -CS sample (figure 6c), this decrease is not visible due to overlapping with the inorganic semiconductor's absorption edge. The transition corresponding to one electron excitation from the ground to the lowest single texticed

state of Chl α (Qy band) [51–54] is observed at approximately 660 nm and the HOMO (highest occupied molecular orbital)–LUMO (lowest unoccupied molecular orbital) energy gap is calculated at 1.9 eV (E_g^2), in all cases. The absorption increase attributed to the Soret-band is also noted in the blue wavelength region of the spectra (figure 6c and f). Finally, Crt-containing samples also exhibit two additional transitions, the first of which, at about 2.2–2.5 eV, corresponds to the one-photon allowed transition from the HOMO to LUMO levels of the Crt molecules (E_g^2) [55–59].

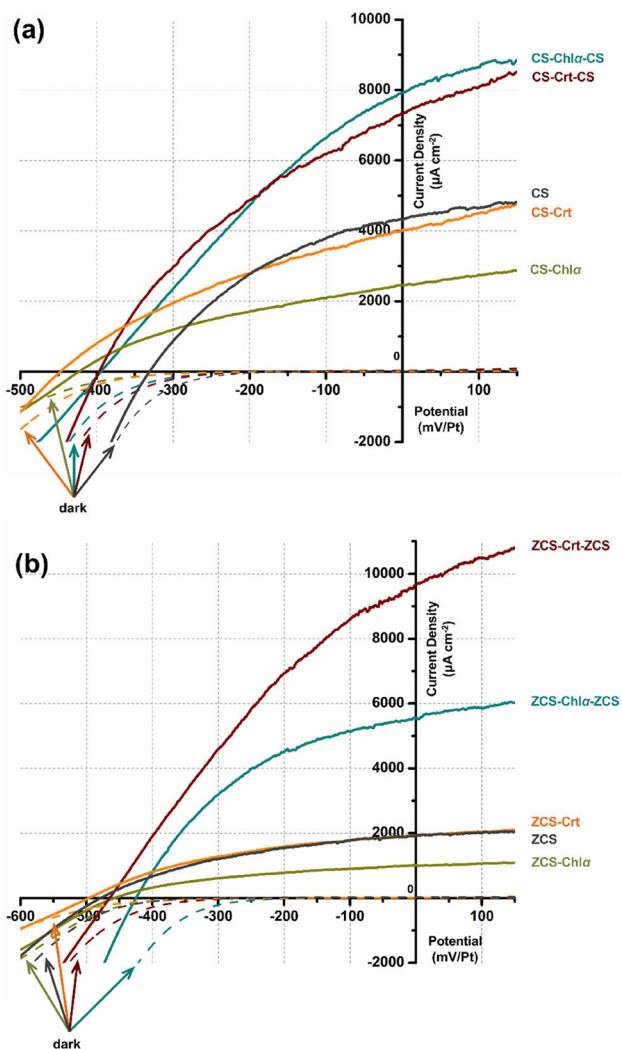


Figure 8. Current density vs. electrochemical potential ('photocurve') given by (a) CdSe-based hybrid and inorganic thin films and (b) Zn_xCd_{1-x}Se-based hybrid and inorganic thin films, used as absorbing electrodes in a photoelectrochemical cell under 1000 W m⁻² illumination and in the dark.

Examining the current–potential photoresponse curves of all hybrid and inorganic thin films that are illustrated in figure 8, it is evident that all photocurrents are anodic and the synthesized semiconductors exhibit an *n*-type semiconducting behaviour. Table 5 summarizes the photoelectrochemical parameters (circuit current density (J_{sc}), open circuit voltage (V_{oc}), fill factor (FF) and photoelectrochemical efficiency ($\eta\%$)) for all inorganic and hybrid samples synthesized and presented in the context of this work.

According to the data collected, the three-layer hybrid deposits, both with Chl α and Crt, exhibit significantly improved J_{sc} and $\eta\%$ values, compared to the respective CdSe and Zn_xCd_{1-x}Se inorganic specimens (refer to table 5). It is extremely important to note that this enhancement is

Table 5. Overview of photoelectrochemical parameters of the synthesized inorganic and hybrid thin films.

Sample abbrev.	J_{sc} ($\mu\text{A cm}^{-2}$)	V_{oc} (mV)	FF	η (%)
CS	4310.27	-330.96	0.39	0.56
CS-Chl α	2463.01	-423.43	0.37	0.39
CS-Chl α -CS	7923.77	-394.59	0.30	0.95
CS-Crt	4018.33	-447.69	0.34	0.61
CS-Crt-CS	7345.82	-396.88	0.35	1.02
ZCS	1926.36	-478.36	0.40	0.37
ZCS-Chl α	1007.08	-457.31	0.40	0.19
ZCS-Chl α -ZCS	5549.88	-424.80	0.42	1.00
ZCS-Crt	1925.85	-496.67	0.40	0.39
ZCS-Crt-ZCS	9668.40	-464.63	0.33	1.46

more prominent in the case of Zn_xCd_{1-x}Se hybrid systems (reaching up to 300% when combined with Crt in ZCS-Crt-ZCS sample), where a significant amount of Cd has been substituted by Zn and, thus, considered to be an environmentally friendlier alternative to pure CdSe-based semiconductors. Also, a 'sandwich-like' structure seems to be necessary in order to receive high-efficiency products, as the double-layered specimens synthesized, examined and presented (figure 8 and table 5) exhibit unaltered or reduced J_{sc} and $\eta\%$ values.

Chlorophyll α and Carotenes have a leading role in native photosynthesis, actively contributing to light-harvesting, as well as in electron and energy transduction processes essential to plants [60–64]. It is assumed that these natural pigments function as electron donors to the hybrid systems, facilitating charge transfer and separation processes at the same time, in correspondence with their role in nature [65–67].

4. Conclusions

In conclusion, hybrid (organic–inorganic) semiconductive systems using natural organic photosynthetic dyes were synthesized. Chlorophyll α or Carotenes were applied as an intermediate layer in CdSe and Zn_xCd_{1-x}Se thin film multi-layered structures, so as to create alternative, biologically inspired solar energy conversion systems. These particular dyes were selected based on the fact that they are abundant and non-toxic natural compounds, involved in energy collection, electron transport and charge separation in natural systems. Owing to their interesting properties and electron-donating character, their introduction to the hybrid system led to improved photoelectrochemical performance in photoelectrochemical studies regarding all CdSe and Zn_xCd_{1-x}Se three-layered thin films that were developed. In the case of the 'sandwich'-type semiconductive systems involving Zn_xCd_{1-x}Se and Carotenes (layer structure: Zn_xCd_{1-x}Se-Crt-Zn_xCd_{1-x}Se), a photoelectrochemical

efficiency increase of 300% was achieved, compared to the corresponding inorganic thin film. Additionally, the incorporation of Zn (20–30%) in the higher performance products, combined with the natural origin of the organic dyes, is a step towards producing low-cost and environmentally friendlier hybrid semiconductors. Given the wide variety of natural compounds with particular photochemical properties, large groups of organic molecules originating from natural sources is possible to be exploited in relevant systems in the near future.

References

- [1] Ebhota W S and Jen T-C 2019 in *Recent developments in photovoltaic materials and devices* N Prabaharan, M A Rosen and P E Campana (ed) (London, UK: IntechOpen) p 43
- [2] Kabir E, Kumar P, Kumar S, Adelodun A A and Kim K-H 2018 *Renew. Sustain. Energy Rev.* **82** 894
- [3] Kumara N T R N, Lim A, Lim C M, Petra M I and Ekanayake P 2017 *Renew. Sustain. Energy Rev.* **78** 301
- [4] Mitzithra C, Kaniaris V, Hamilakis S, Kordatos K, Kollia C and Loizos Z 2011 *Mater. Lett.* **65** 1651
- [5] Chandramohan R, Hsu L-S, Thanikaikarasan S, Raja M, Kumar K and Mahalingam T 2006 *Proc. SPIE* 60290 p 60290M
- [6] Manivannan R and Noyel Victoria S 2018 *Sol. Energy* **173** 1144
- [7] Mir S H, Nagahara L A, Thundat T, Mokarian-Tabari P, Furukawa H and Khosla A 2018 *J. Electrochem. Soc.* **165** B3137
- [8] Werwie M, Dworak L, Bottin A, Mayer L, Basché T, Wachtveitl J *et al* 2018 *Biochim. Biophys. Acta—Bioenerg.* **1859** 174
- [9] Hu G, Liu R, Alexy E J, Mandal A K, Bocian D F, Holten D *et al* 2016 *New J. Chem.* **40** 8032
- [10] Passalacqua R, Perathoner S and Centi G 2017 *J. Energy Chem.* **26** 219
- [11] Yfanti-Katti M, Prokopos-Chouliaras F, Milonakou-Koufoudaki K, Mitzithra C, Kordatos K, Hamilakis S *et al* 2017 *Semiconductors* **51** 1592
- [12] Milonakou-Koufoudaki K, Lyros T, Mitzithra C, Hamilakis S, Kollia C and Loizos Z 2017 *J. Appl. Electrochem.* **47** 1023
- [13] Aery N C and Jagetiya B L 1997 *Commun. Soil Sci. Plant Anal.* **28** 949
- [14] Scoullou M J, Vonkeman G H, Thornton I and Makuch Z 2001 M J Scoullou (ed) *Mercury–cadmium–lead handbook for sustainable heavy metals policy and regulation* (Dordrecht: Springer Science + Business Media, B.V.)
- [15] Attar E N and Maly E J 1982 *Arch. Environ. Contam. Toxicol.* **11** 291
- [16] Dikio E D and Isabirye D A 2008 *Bull. Chem. Soc. Ethiop.* **22** 301
- [17] Bakker H A 1934 *Proc. Akad. Wet. Amsterdam* **37** 679
- [18] Lichtenthaler H K 1987 *Methods Enzymol.* **148** 350
- [19] Jeyanthi Rebecca L, Sharmila S, Das M P and Seshiah C 2014 *J. Chem. Pharm. Res.* **6** 594
- [20] Bhattacharya A, Biswas P, Kar P, Roychoudhury P, Basu S, Ganguly S *et al* 2017 *Anal. Chim. Acta* **985** 101
- [21] Iriyama K, Shiraki M and Yoshiura M 1979 *J. Liq. Chromatogr.* **2** 255
- [22] Khalyfa A, Kermasha S and Alli I 1992 *J. Agric. Food Chem.* **40** 215
- [23] Jinasena M A M, Amarasinghe A D U S, Amarasinghe B M W P K and Prashantha M A B 2016 *J. Natl. Sci. Found. Sri Lanka* **44** 11
- [24] Sumanta N, Haque C I, Nishika J and Suprakash R 2014 *Res. J. Chem. Sci.* **4** 63
- [25] Lichtenthaler H K and Buschmann C 2001 *Curr. Protoc. Food Anal. Chem.* **1** F4.3
- [26] Boyer R F 1990 *Biochem. Educ.* **18** 203
- [27] Kumar P, Singh J, Pandey M K, Jeyanthi C E, Siddheswaran R, Paulraj M *et al* 2014 *Mater. Res. Bull.* **49** 144
- [28] Borah M N, Baruah B J, Chaliha S, Gogoi D P, McFarlane U and Dutta S 2013 *J. Exp. Nanosci.* **8** 273
- [29] Girija K, Thirumalairajan S, Mohan S M and Chandrasekaran J 2009 *Chalcogenide Lett.* **6** 351
- [30] Sarmah K, Sarma R and Das H L 2008 *Chalcogenide Lett.* **5** 153
- [31] Sarmah K, Sarma R and Das H L 2009 *J. Non-Oxide Glas.* **1** 143
- [32] Ayeshamariam A, Kashif M, Muthu S, Jagadeswari S, Saravanankumar D, Alhaji N M I *et al* 2014 *Int. J. Emerg. Technol. Adv. Eng.* **4** 584
- [33] Peñuelas J and Filella I 1998 *Trends Plant Sci.* **3** 151
- [34] Basayigit L, Ersan R and Dedeoglu M 2013 *Bulg. J. Agric. Sci.* **19** 1219
- [35] Sengupta D, Mondal B and Mukherjee K 2015 *Spectrochim. Acta Part A Mol. Biomol. Spectrosc.* **148** 85
- [36] Zhang J, Han W, Huang L, Zhang Z, Ma Y and Hu Y 2016 *Sensors* **16** 437
- [37] Salem A, Saion E, Al-Hada N M, Kamari H M, Shaari A H and Radiman S 2017 *Results Phys.* **7** 1175
- [38] López R and Gómez R 2012 *J. Sol–Gel Sci. Technol.* **61** 1
- [39] Abdullahi S S, Güner S, Koseoglu Y, Murtala I, Adamu B I and Abdulhamid M I 2016 *J. NAMP* **35** 241
- [40] Escobedo Morales A, Sanchez Mora E and Pal U 2007 *Rev. Mex. Física* **53** 18
- [41] Lee H K, Talib Z A, Mamat Mat Nazira M S, Wang E, Lim H N, Mahdi M A *et al* 2019 *Materials (Basel)* **12** 2295
- [42] Shlyk L, Strobel S, Farmer B, De Long L E and Niewa R 2018 *Phys. Rev. B* **97** 054426
- [43] Friedrich D, Schlosser M, Wehrich R and Pfitzner A 2017 *Inorg. Chem. Front.* **4** 393
- [44] Hamden Z, Conceição D, Boufi S, Vieira Ferreira L and Bouattour S 2017 *Materials (Basel)* **10** 600
- [45] Suram S K, Newhouse P F and Gregoire J M 2016 *ACS Comb. Sci.* **18** 673
- [46] Savory C N, Ganose A M, Travis W, Atri R S, Palgrave R G and Scanlon D O 2016 *J. Mater. Chem. A* **4** 12648
- [47] Escobedo-Morales A, Ruiz-López I I, Ruiz-Peralta M de L, Tepech-Carrillo L, Sánchez-Cantú M and Moreno-Orea J E 2019 *Heliyon* **5** e01505
- [48] Baranoski G V G and Rokne J G 2005 *Int. J. Remote Sens.* **26** 503
- [49] Xie Q, Dash J, Huang W, Peng D, Qin Q, Mortimer H *et al* 2018 *IEEE J. Sel. Top. Appl. Earth Obs. Remote Sens.* **11** 1482
- [50] Curran P J, Windham W R and Gholz H L 1995 *Tree Physiol.* **15** 203
- [51] Gruber E, Kjær C, Nielsen S B and Andersen L H 2019 *Chem.—A Eur. J.* **25** 9153

- [52] Blankenship R E, Tiede D M, Barber J, Brudvig G W, Fleming G, Ghirardi M *et al* 2011 *Science* **332** 805
- [53] Kosumi D, Nishiguchi T, Amao Y, Cogdell R J and Hashimoto H 2018 *J. Photochem. Photobiol. A Chem.* **358** 374
- [54] Senge M, Ryan A, Letchford K, MacGowan S and Mielke T 2014 *Symmetry* **6** 781
- [55] Polivka T, Herek J L, Zigmantas D, Akerlund H-E and Sundstrom V 1999 *Proc. Natl. Acad. Sci.* **96** 4914
- [56] Pazhanivel T, Nataraj D, Devarajan V P, Senthil K, Seol M and Yong K 2012 *Appl. Phys. Lett.* **100** 261110
- [57] Zigmantas D, Hiller R G, Sundstrom V and Polivka T 2002 *Proc. Natl. Acad. Sci.* **99** 16760
- [58] Flores-Hidalgo M, Torres-Rivas F, Monzon-Bensojo J, Escobedo-Bretado M, Glossman-Mitnik D and Barraza-Jimenez D 2017 in *Carotenoids* D J Cvetkovic and G S Nikolic (ed) (London, UK: IntechOpen) p 17
- [59] Wei-Long L, De-Min W, Zhi-Ren Z, Ai-Hua L and Wen-Hui S 2010 *Chin. Phys. B* **19** 013102
- [60] Green B R and Durnford D G 1996 *Annu. Rev. Plant Physiol. Plant Mol. Biol.* **47** 685
- [61] Telfer A 2002 *Philos. Trans. R Soc. Lond. Ser. B Biol. Sci.* **357** 1431
- [62] Faller P, Pascal A and Rutherford A W 2001 *Biochemistry* **40** 6431
- [63] Young A J and Frank H A 1996 *J. Photochem. Photobiol. B Biol.* **36** 3
- [64] Kargul J and Barber J 2008 *FEBS J.* **275** 1056
- [65] Boussaad S, Tazi A and Leblanc R M 1997 *Proc. Natl. Acad. Sci.* **94** 3504
- [66] Das D, Sarkar Manna J and Mitra M K 2015 *J. Phys. Chem. C* **119** 6939
- [67] Mairanovskii V G, Engovatov A A, Ioffe N T and Samokhvalov G I 1976 *Pharm. Chem. J.* **10** 1238